The Erk2 MAPK Regulates CD8 T Cell Proliferation and Survival[1]

Warren N. D'Souza,[2] Chiung-Fang Chang, April M. Fischer, Manqing Li, and Stephen M. Hedrick[3]

The magnitude of T cell responses is determined by proliferation and survival decisions made by the responding cells. We now demonstrate that the Erk MAPK pathway plays a critical role in these cell fate decisions within CD8 T cells. While Erk1 is dispensable for all aspects of CD8 T cell activation, Erk2 is required for the proliferation of CD8 T cells activated in the absence of costimulation. Surprisingly, Erk2 is not required for proliferation following the addition of a costimulatory signal in vitro, or upon viral infection in vivo, but regulates the size of the responding population by enhancing cell survival. An important component of this Erk2-derived signal is the transcriptional regulation of Bcl-2 family members Bcl-x_L and Bim, and impaired Erk2-deficient CD8 T cell survival can be rescued by genetic ablation of Bim. These studies ascribe multifaceted functions specific to Erk2 in CD8 T cell activation, proliferation, and survival. *The Journal of Immunology,* **2008, 181: 7617–7629.**

Naive T cells are activated via TCR-mediated recognition of antigenic peptides complexed to the appropriate MHC molecules. Upon activation, these cells proliferate rapidly and can undergo up to a 10^5-fold expansion within a period of a week to generate an impressive number of effector T cells (1–3). In addition to proliferation, survival vs death decisions that are made by responding Ag-specific T cells during this expansion phase are critical in determining the outcome of the T cell response. These diverse cell fate choices are the result of a summation of different signaling pathways initiated at the T cell surface, and the activation of the MAPK cascades is thought to be key in this regard (4).

The MAPKs are evolutionary conserved molecules that regulate key cellular functions such as movement, metabolism, growth, survival, proliferation, and differentiation in a variety of different cell types. The Erks were the first members of the MAPK family to be identified (5), and since then at least three additional members have been characterized. These include the stress-activated protein kinases (Sapk) or Jnk, p38 kinases, and Erk5 (6). Erk1 (Mapk3) and Erk2 (Mapk1) are the two main isoforms of the prototypical MAPK Erk. They are ubiquitously expressed serine/threonine kinases that exhibit >80% homology, are regulated in a similar manner, and have been shown to phosphorylate common substrates (7). However, despite the fact that these two kinases appear functionally similar and are thought to be interchangeable, the phenotype of mice deficient in either one of these molecules is very different. *Erk1*$^{-/-}$ mice are viable and phenotypically normal (8), whereas even a hemizygous Erk2 deficiency can result in embryonic lethality (9–12). This may be due to differences in the relative levels of Erk1 and Erk2 in different tissues or due to functional differences between these two isoforms (13, 14).

Erk1 and Erk2 are activated in T cells following TCR triggering by a well-studied signaling cascade that involves the sequential activation of the small GTPase Ras, recruitment and activation of Raf-1, phosphorylation of Mek1 and Mek2, and dual phosphorylation of Erk1/2 (7, 15, 16). Studies using pharmacological inhibitors of the Ras-Erk cascade or mice defective in signaling components upstream of Erk led to the conclusion that Erk was responsible for the differentiation of developing thymocytes during the process of positive selection (15, 17–22). Consistent with this hypothesis, the original description of the *Erk1* knockout mouse indicated that the absence of Erk1 resulted in impaired positive selection (8); however, it has since been shown that Erk1 does not play a major role in positive selection and that the presence of Erk2 is more important for T cell progression through multiple developmental checkpoints, including positive selection (9, 23).

The Erk pathway is also induced by growth-promoting or mitogenic signals (24) and is necessary for G_1 to S phase progression in a variety of cell types (25). It has been demonstrated that Mek1/2 inhibitors are capable of inhibiting proliferation of immature and mature T cells in vitro (26, 27). While the initial characterization of *Erk1*-deficient mice led to the conclusion that proliferation of thymocytes in vitro was defective in the absence of Erk1 (8), thymocytes expressing a dominant-negative Mek protein were shown to proliferate normally (22). Additionally, use of *Erk1*-deficient mice to study the specific requirement for this kinase in supporting mature CD4 T cell proliferation has yielded contradictory results, with some studies suggesting that proliferation of CD4 T cells in vitro is defective (28) while others have demonstrated normal activation and proliferation (23). Thus, the importance of Erk in mature T cell proliferation is unclear and, more importantly, the relative roles for Erk1 vs Erk2 in this regard remain unknown.

T cell expansion is typically followed by a contraction phase wherein most of the effector cells undergo apoptosis. T cell apoptosis following acute antigenic stimulation in vivo is primarily the result of an intrinsic apoptosis pathway triggered by a disruption in

Molecular Biology Section, Division of Biological Science, and the Department of Cellular and Molecular Medicine, University of California, San Diego, La Jolla, CA 92093

Received for publication July 2, 2008. Accepted for publication September 30, 2008.

The costs of publication of this article were defrayed in part by the payment of page charges. This article must therefore be hereby marked *advertisement* in accordance with 18 U.S.C. Section 1734 solely to indicate this fact.

[1] These studies were supported by a fellowship from the Leukemia and Lymphoma society (to W.N.D.) and National Institutes of Health Grant 5R01 AI021372-25 (to S.M.H.).

[2] Current address: Amgen Inc., One Amgen Center Drive, Thousand Oaks, CA 91320.

[3] Address correspondence and reprint requests to Dr. Stephen M. Hedrick, Division of Biological Sciences, University of California, San Diego, 9500 Gilman Drive, La Jolla, CA 92093-0377. E-mail address: shedrick@ucsd.edu

the integrity of the mitochondrial outer membrane, and members of the Bcl-2 family of proteins are critical regulators of this pathway (29, 30). The Bcl-2 family can be subdivided into three groups of proteins (31): prosurvival members containing the BH1–4 domains (Bcl-2, Bcl-x_L, Bcl-w, A1, and Mcl1), proapoptotic members containing the BH1–3 domains (Bax, Bak, and Bok), and, lastly, another group of proapoptotic molecules that only contain the BH3 domain (Bim/Bod, Bad, Bik, Bid, Bmf, Hrk, Noxa, and Puma). It appears that the ratio of Bcl-2 and Bcl-x_L to that of Bim plays a key role in regulating the survival of T cells (32–34), but there is no consensus with regard to the mechanism underlying the ability of Bim to mediate T cell apoptosis. For instance, while cell viability in certain cell types is maintained via the sequestration of Bim to the microtubular dynein motor complex (35), Bim is normally associated with Bcl-2 and Bcl-x_L on the mitochondria of healthy T cells (36). Additionally, it has been reported that Bim levels are up-regulated following T cell activation (37), but other studies have led to the conclusion that Bim levels do not change appreciably within activated T cells (33, 34). Thus, the current notion is that T cell death following acute antigenic stimulation occurs primarily due to a reduction in the levels of Bcl-2 and Bcl-x_L (30).

In this report, we investigated the roles played by Erk1 and Erk2 in the proliferation and survival/death decisions that are made following CD8 T cell activation. We observed that Erk1 was largely dispensable for CD8 T cell proliferation and survival. On the other hand, Erk2 was required for cell cycle initiation in the absence of costimulation, but not following activation with anti-CD3 and anti-CD28 in vitro or viral infections in vivo. Under these conditions, Erk2 was found to determine the magnitude of clonal expansion by regulating the rate of CD8 T cell death.

Materials and Methods

Mice and pathogens

C57BL/6J and *Bim*$^{-/-}$ mice were obtained from The Jackson Laboratory. We have previously reported the generation of mice harboring the *Erk2* conditional allele (9). The *Erk1*$^{-/-}$ mice and the dLck-icre mice were kindly provided by Dr. Giles Pages (Nice, France) and Dr. Nigel Killeen (University of California, San Francisco), respectively. For adoptive transfer experiments, lymphocytes isolated from lymph nodes of wild-type (WT)[4] *OT-I*$^{+}$ or *OT-I*$^{+}$*Erk2*$^{T-/-}$ mice were injected i.v. into naive congenic B6.PL (CD45.1^{+}) mice. In some experiments, donor cells were labeled with CFSE (Invitrogen) before transfer. For in vivo elicitation of T cell responses, mice were infected i.p. with 2×10^5 PFU lymphocytic choriomeningitis virus (LCMV-Armstrong), i.v. with 1×10^5 PFU vesicular stomatitis virus (VSV-Indiana), or with VSV-expressing OVA (VSV-OVA), as indicated. VSV strains were kindly provided by Dr. Leo Lefrançois (University of Connecticut Health Center). All mice used (except for the *Bim*$^{-/-}$ and *Erk2*$^{T-/-}$Bim$^{-/-}$ mice) had been backcrossed to the C57BL/6 background for eight generations or more. The mice were housed and bred at University of California, San Diego, and all animal work was performed in accordance with the institutional guidelines.

Flow cytometry

Lymphocytes were isolated from PBL, lymph nodes, or spleen, and single-cell suspensions were prepared. Cells from PBL and spleen were subjected to RBC lysis using ACK lysis buffer. Approximately 1–2 million cells were then resuspended in FACS buffer and stained with fluorescently conjugated Abs or MHC class I tetramers. For several of the in vitro studies, equal volumes of harvested cells were stained, resuspended in identical volumes of FACS buffer, and run for a fixed amount of time on the FACS. In some experiments, cells were also stained with recombinant human annexin V-PE (Caltag Laboratoties) before analysis by FACS. In other experiments, harvested cells were fixed and permeabilized with 70% ethanol, treated with RNase, labeled with propodium iodide, and analyzed by FACS. All Abs were purchased from BD Pharmingen or eBioscience, and MHC class I tetramers were kindly provided by Dr. Vaiva Vezys and Dr. David Masopust (University of Minnesota) and the National Institutes of Health Tetramer Facility. The data were collected on a FACSCalibur (BD Biosciences) and analyzed using FlowJo software (Tree Star). Cell cycle analyses using propidium iodide (PI) were also performed using ModFit LT software (Verity Software House).

CD8 T cell purification, CFSE labeling, and in vitro stimulation

Single-cell suspensions were made from lymph nodes and spleens. CD8 T cells were purified by positive or negative selection using magnetic beads (Miltenyi Biotec). Purified T cells were labeled with CFSE by suspending them at a concentration of 10×10^6 per ml in HBSS containing 1 μM CFSE for 10 min at 37°C. In vitro stimulation assays were performed by plating cells in anti-CD3-coated (2.5 ng/well) tissue culture plates. Soluble anti-CD28 (BD Pharmingen) or recombinant human IL-2 (20 U/ml) was also added to wells as indicated. For analyses of IL-2 levels, culture supernatants were harvested at indicated time points and measured using an IL-2 ELISA kit (eBioscience) as per the manufacturer's instructions. In some experiments cells were stimulated with PMA for 15 min, while in others analyzing very early time points postactivation, T cells were activated by adding biotin-labeled anti-CD3 in the presence of anti-CD28, followed by streptavidin crosslinking.

Intracellular IFN-γ staining

For detection of intracellular cytokines, splenocytes were isolated at day 8 postinfection. They were then cultured with LCMV-derived peptide $NP_{396-404}$ in the presence of monensin (BD Pharmingen) for 5 h. Cells were stained for cell surface Ags, fixed, and permeabilized to detect intracellular IFN-γ according to the manufacturer's instructions (BD Pharmingen).

Measurement of cytolytic activity

Cytolytic activity was measured using ^{51}Cr-labeled EL4 cells as targets, with the addition of LCMV glycoprotein-derived peptide. Serial dilutions of effector cells isolated from day 8 LCMV-infected mice (or unimmunized controls) were incubated in 96-well round-bottom plates with 2.5×10^3 target cells for 4 h at 37°C. Percentage specific lysis was calculated as: $100 \times$ [(cpm released with effectors) − (cpm released alone)]/[(cpm released with detergent) − (cpm released alone)]. Data were also corrected for the actual number of peptide-specific CD8 T cells present in each well, based on staining with MHC class I tetramers.

SDS-PAGE and Western blotting

Cells were lysed in a buffer containing 1% Nonidet P-40, 150 mM NaCl, and 50 mM Tris with protease and phosphatase inhibitors (Calbiochem). Protein concentrations were estimated using the Lawry method. Equal amounts were run on 12% SDS-PAGE gels (Invitrogen) and transferred to a polyvinylidene difluoride membrane (Millipore) using a semidry transfer cell (Bio-Rad). Blots were blocked and incubated with the primary Ab at 4°C overnight, or at room temperature for 2 h. The appropriate HRP-conjugated secondary Ab was then added for 30 min at room temperature and ECL was used to visualize the proteins. The following primary Abs were used: anti-Erk1/2 (Santa Cruz Biotechnology and Zymed Laboratories), anti-Bim (Sigma-Aldrich), anti-Bcl-2 (BD Biosciences), anti-Bcl-x_L (Cell Signaling Technology), Zap70 (BD Biosciences), and PLCγ (Millipore/Upstate Biotechnology). The secondary HRP-conjugated Abs were obtained from Vector Laboratories or SouthernBiotech. The anti-pS65 Bim primary Ab was generously provided by Dr. Hisashi Harada (Virginia Commonwealth University). For phosphatase treatment, cells were lysed in lysis buffer not containing phosphatase inhibitors. and lysates were then incubated with 20 U of calf intestinal phosphatase in the presence of magnesium for 1 h at 37°C.

BrdU incorporation studies

Mice were injected i.p. with 1 mg of BrdU in PBS. Mice were sacrificed at indicated time points and spleens were harvested. Single-cell suspensions of splenocytes were surface stained with Abs and MHC class I tetramers as described above and then analyzed for BrdU incorporation using a modified procedure of the BD Biosciences BrdU flow kit. In brief, the stained cells were suspended in BD Cytofix/Cytoperm, washed, and stored at −80°C in freezing media. The next day, the cells were thawed and incubated in BD Cytofix/Cytoperm, treated with DNase, stained with anti-BrdU Abs, and analyzed by FACS.

[4] Abbreviations used in this paper: WT, wild type; LCMV, lymphocytic choriomeningitis virus; PI, propidium iodide; VSV, vesicular stomatitis virus; VSV-OVA, VSV-expressing OVA.

RNA isolation, microarray analyses, and real-time quantitative PCR

RNA was isolated using TRIzol (Invitrogen) or RNeasy (Qiagen) as per the manufacturers' instructions, and treated with DNase (DNA-free kit, Ambion). Microarray analyses were performed by the University of California, San Diego microarray core using the Agilent Mouse 4 × 44K array. These data have been deposited in the European Bioinformatics Institute (EBI) ArrayExpress database (www.ebi.ac.uk/microarray-as/ae/), and the accession number is E-MEXP-1833. For real-time quantitative PCR analyses, extracted RNA was reverse-transcribed using random hexamers and SuperScript III reverse transcriptase (Invitrogen) and the cDNA was amplified and detected using an Mx3005P machine and SYBR Green (Stratagene). Samples were analyzed after normalization to GAPDH or Cph (cyclophilin A). Cph was used as the housekeeping gene in all experiments analyzing a time course of gene expression. As indicated in the figure legends, the levels of gene expression in the Erk-deficient cells were further normalized to the WT controls. The following sets of primer pairs were used: Bim_{EL}: forward, GCCCTGGCCCTTTTGC, reverse, CCGGGAC AGCAGAGAAGATC; Bim_L: forward, GACAGAACCGCAAGACAG GAG, reverse, TGGCAAGGAGGACTTGGG; Bim_S: forward, TGCGC CCGGAGATACG, reverse, TTCGTTGAACTCGTCTCCGA; *Bcl2*: forward, ACTTCGCAGAGATGTCCAGTCA, reverse, TGGCAAAGC GTCCCCTC; *Bcl-x*$_L$: forward, GAATGGAGCCACTGGCCA, reverse, GCTGCCATGGGAATCACCT; *Gapdh*: forward, CCAGTATGACTC CACTCACG, reverse, GACTCCACGACATACTCAGC; *Cph*: forward, CACCGTGTTCTTCGACATC, reverse, ATTCTGTGAAAGGAG GAACC.

Results

Erk1 is dispensable for CD8 T cell activation and proliferation

The Erk proteins are necessary for G_1 to S phase progression in a variety of cell types (25), and studies using Mek inhibitors have pointed to a similar role for them within T cells (26, 27). There are conflicting data with regard to the role for Erk1 in mature CD4 T cell activation and proliferation (8, 23), and the function for either Erk1 or Erk2 within mature CD8 T cells remains unknown. Thus, we first examined the effect of an Erk1 deficiency on CD8 T cell activation and proliferation. To visualize cell division, purified CD8 T cells from WT or *Erk1*-deficient ($Erk1^{-/-}$) mice were labeled with CFSE. The cells were cultured in vitro without stimulation or were activated by plate-bound anti-CD3 in the presence or absence of a costimulatory signal, anti-CD28. Cells were harvested at various time points and cell division was assayed by CFSE dilution while survival was assayed using trypan blue exclusion (data not shown) and flow cytometry (Fig. 1*A*). We did not observe a difference in CFSE dilution or cell accumulation between the $Erk1^{-/-}$ CD8 T cells and the WT controls at any of the time points and under all conditions tested (Fig. 1*A* and data not shown). These results demonstrate that Erk1 is largely dispensable for naive CD8 T cell survival in vitro and for CD8 T cell proliferation and survival following activation.

We then determined the in vivo requirement for Erk1 in CD8 T cell responses by infecting WT or $Erk1^{-/-}$ mice with LCMV and measuring the CD8 T cell response to the NP_{396} epitope of LCMV using MHC class I tetramers. We did not observe a difference in the proportion or number of Ag-specific CD8 T cells that were generated at the peak of the primary response to LCMV in the absence of Erk1 (Fig. 1*B*). Thus, consistent with the in vitro results, Erk1 was also dispensable for CD8 T cell proliferation and survival in vivo.

Erk2$^{f/f}$dLck-icre *mice possess normal T cell compartments*

We next analyzed the contribution of signals derived from Erk2 to peripheral CD8 T cell activation. Using mice harboring *loxP*-flanked *Erk2* alleles ($Erk2^{f/f}$) and a Cre recombinase transgene driven by the *Cd4* promoter (*Cd4*Cre), we previously demonstrated that Erk2 regulates multiple stages of T development (9). Although mature T cells were present within the secondary lymphoid tissues

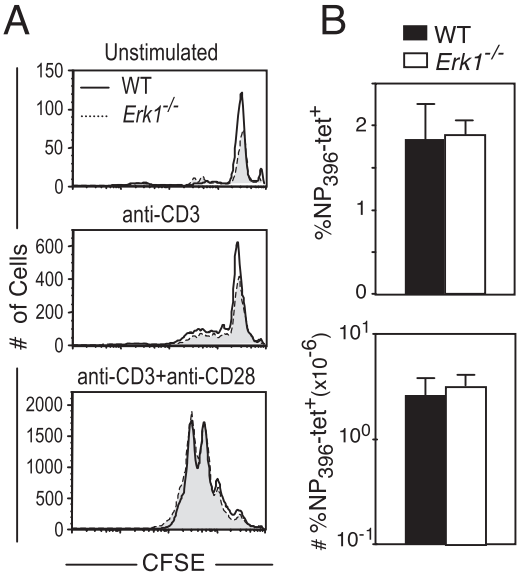

FIGURE 1. Erk1 is dispensable for CD8 T cell activation and proliferation. *A*, WT (unshaded histograms) or $Erk1^{-/-}$ (shaded histograms) CD8 T cells were labeled with CFSE and were left unstimulated or were stimulated in vitro for 3 days with plate-bound anti-CD3 with or without the addition of soluble anti-CD28. CFSE profiles are gated on $CD8^+$ cells, and the actual number of cells run on the FACS in a fixed period is plotted. *B*, WT and $Erk1^{-/-}$ mice infected i.p. with LCMV and Ag-specific CD8 T cells within the spleen were assayed at day 8 postinfection using H-$2D^b$-NP_{396} tetramers, and the size of responding population was plotted as a proportion of lymphocytes or absolute number of cells present within the spleen. The data presented are the means ± SD and are representative of three independent experiments.

of these animals, it was possible that they had developed abnormally. Thus, we bred the $Erk2^{f/f}$ mice to transgenic mice expressing the Cre recombinase under the control of the distal promoter of the mouse *Lck* gene (*dLck-icre*) (38). Here, Cre expression is initiated in thymocytes after positive selection, and by generating $Erk2^{f/f}$*dLck-icre*$^+$ ($Erk2^{T-/-}$) mice, we obtained mature T cells that deleted the *Erk2* gene after having undergone normal thymic selection. We first examined the CD4 and CD8 T cell compartments present within the primary and secondary lymphoid organs of these animals (Fig. 2*A*). $Erk2^{f/f}$ and $Erk2^{+/+}$*;dLckCre*$^+$ mice exhibited no differences compared with WT mice ($Erk2^{+/+}$*;dLck-icre*$^-$), and they were pooled as littermate controls. The thymii and spleens of the $Erk2^{T-/-}$ mice were indistinguishable from those of the control littermates (Fig. 2*A*). For unknown reasons, the peripheral lymph nodes of the $Erk2^{T-/-}$ mice consistently displayed increased cellularity and a smaller proportion of T cells (Fig. 2*A*). However, the net result was a similar number of CD4 and CD8 T cells in the lymph nodes when compared with WT mice. We examined the proportion of naive and effector/memory T cells within secondary lymphoid tissue by analyzing the expression of the activation markers CD62L and CD44. We observed no difference in the proportion of $CD62L^{low}$ CD4 and CD8 T cells (data not shown), but there was a slight but consistent increase in the proportion of $CD44^{high}CD8^+$ T cells, particularly in the spleens of the $Erk2^{T-/-}$ animals (Fig. 2*B*). The proportion of T cells expressing markers of recently activated cells such as CD25 and CD69 were comparable between the WT and $Erk2^{T-/-}$ mice (data not shown). Thus, $Erk2^{T-/-}$ mice appeared normal for the most part, and the finding that the thymus composition was unaltered confirmed that *Erk2* was not deleted before positive selection. To determine whether *Erk2* was deleted within the peripheral T cells, we purified

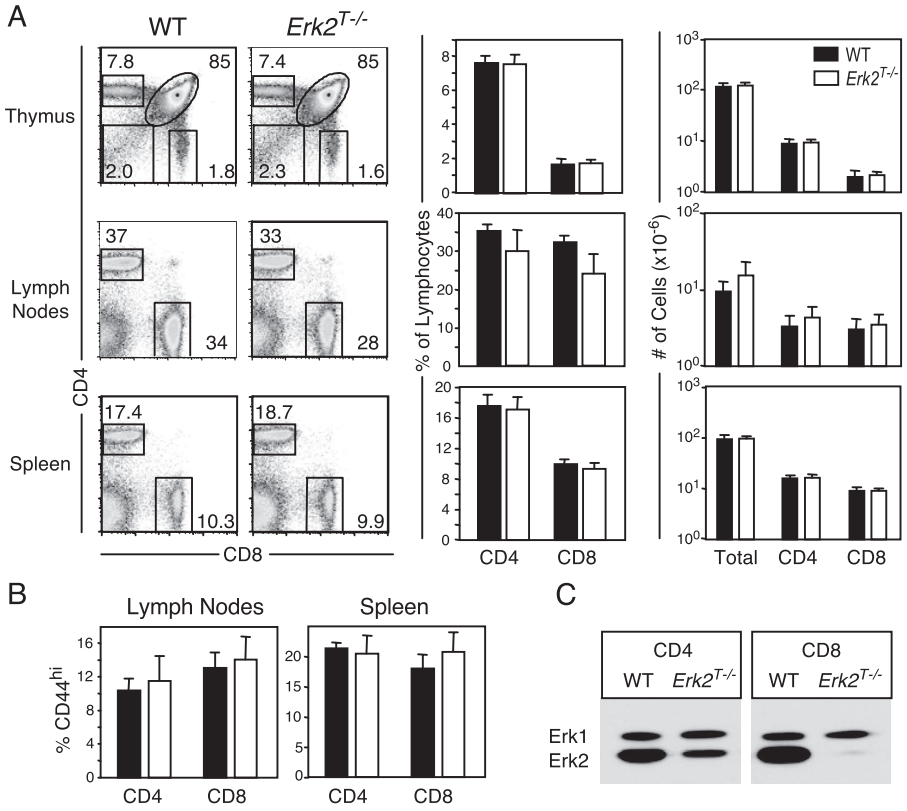

FIGURE 2. *Erk2$^{f/f}$dLck-icre* mice possess normal T cell compartments. *A*, Lymphocytes within the thymus, lymph nodes, and spleens of 12–13-wk-old *Erk2$^{T-/-}$* (*Erk2$^{f/f}$*Cre^{+}, open bars) and control (*Erk2$^{f/f}$*Cre^{-} or *Erk2$^{+/+}$*Cre^{+}, filled bars) mice were analyzed by flow cytometry. Representative FACS plots and pooled data indicating proportions and absolute numbers of lymphocytes, CD4, and CD8 T cells in indicated compartments are shown. The data presented are the means ± SD. The FACS plots are gated on live lymphocytes, and numbers indicate proportion of the same. *B*, Proportion of CD44^{high} CD4 and CD8 T cells in the lymph nodes and spleens of WT and *Erk2$^{T-/-}$* mice. The data presented are the means ± SD. *C*, Purified CD4 and CD8 T cells from lymph node were analyzed for the presence of Erk1 and Erk2 by Western blotting.

CD4 and CD8 T cells from the lymph nodes and spleens of the *Erk2$^{T-/-}$* mice and subjected them to Western blot analyses (Fig. 2*C*). The studies clearly demonstrated efficient deletion of *Erk2* and elimination of protein within peripheral CD8 T cells and provided us with an ideal system to study peripheral CD8 T cell activation in the absence of Erk2. Consistent with the original description of this 3779 line of dLck-icre mice, deletion was not as efficient within the CD4 T cell subset (38).

Activation of Erk2$^{T-/-}$ *CD8 T cells in vitro*

We determined the requirement for Erk2 in the activation of CD8 T cells following stimulation of the TCR in the absence (anti-CD3 alone) or presence of a costimulatory signal (anti-CD3 + anti-CD28). To this end, CD8 T cells were purified from the secondary lymphoid organs of *Erk2$^{T-/-}$* and WT littermate controls, labeled with CFSE, and were either left unstimulated or were stimulated as indicated. The number of WT and *Erk2$^{T-/-}$* cells recovered from culture when left unstimulated was similar (Fig. 3*A*, *top panels*), suggesting that Erk2 does not regulate naive CD8 T cell survival under resting conditions in vitro. In keeping with the well-defined role for Erk as a master regulator of cell cycle initiation (25), stimulation of CD8 T cells with anti-CD3 alone resulted in markedly reduced proliferation of *Erk2$^{T-/-}$* CD8 T cells when compared with the WT cells (Fig. 3*A*, *middle panels*). This impaired proliferation was also observed when the cells were stimulated with higher concentrations of anti-CD3 or when DNA synthesis as measured by [^{3}H]thymidine incorporation was used as a readout of proliferation (data not shown). Surprisingly, following stimulation with anti-CD3 and anti-CD28, we observed no change in the division profiles on days 1 (data not shown) 2, 3, and 4 (Fig. 3*A*, lower panels) in the absence of Erk2. While the numbers of surviving *Erk2$^{T-/-}$* CD8 T cells appeared identical to those of WT cells on days 1 (data not shown) and 2 (Fig. 3*A*) postactivation, we observed an ~2-fold reduction in *Erk2$^{T-/-}$* CD8 T cell recovery at day 3. This reduced survival was more evident by day 4, when the recovery of *Erk2$^{T-/-}$* cells was substantially diminished compared with WT controls. Identical results with regard to cell recovery and viability were obtained by cell counts and trypan blue exclusion (data not shown). These data pointed to a critical role for Erk2 in maintaining cell survival within proliferating effector CD8 T cells.

We then analyzed early activation events such as the up-regulation of CD25 (IL-2Rα) and CD69 on the surface of the activated CD8 T cells. Stimulation with anti-CD3 alone resulted in the up-regulation of CD69 and CD25 on far fewer *Erk2$^{T-/-}$* cells when compared with the WT cells (Fig. 3*B*). In contrast, following stimulation with anti-CD3 and anti-CD28 (Fig. 3*C*), most WT and *Erk2$^{T-/-}$* CD8 T cells up-regulated CD69 and CD25. However, the levels of these molecules present on the *Erk2$^{T-/-}$* CD8 T cells were lower when compared with those on their WT counterparts at all time points studied. Thus, the relative requirement for Erk2 in supporting CD8 T cell activation, proliferation, and survival was dependent on the nature of the activating stimulus.

Increased death of in vitro activated CD8 T cells in the absence of Erk2

Our results led to the conclusion that the phenotype observed following stimulation of *Erk2$^{T-/-}$* cells with anti-CD3 and anti-CD28 was due to an imbalance of the signals that regulate cell survival vs death. To directly determine whether the *Erk2$^{T-/-}$* CD8 T cells were undergoing apoptosis at an increased rate at later time points, we used annexin V binding to directly visualize the dying cells (Fig. 4*A*). At day 2 poststimulation with anti-CD3 and anti-CD28, we observed few WT and *Erk2$^{T-/-}$* cells that bound annexin V. By day 3, although the number of dying cells had increased in both populations, the *Erk2$^{T-/-}$* cells now exhibited a 2-fold increase compared with the WT cells. We confirmed these results by using PI to measure cell cycling and cell death (Fig. 4*B*).

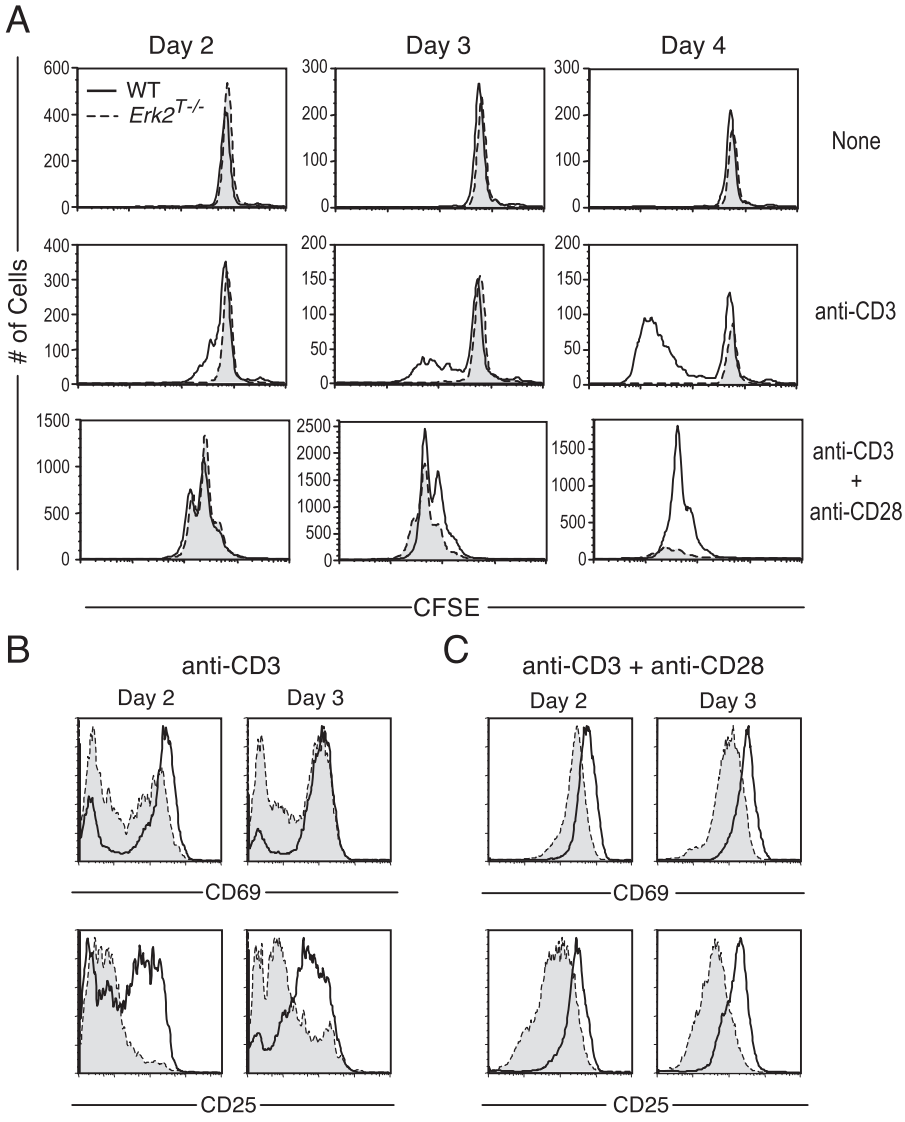

FIGURE 3. Multiple roles for Erk2 in CD8 T cell activation. *A*, Purified CD8 T cells from WT (unshaded histograms) or $Erk2^{T-/-}$ (shaded histograms) mice were labeled with CFSE and left unstimulated or were stimulated in vitro for indicated time points with plate-bound anti-CD3 with or without soluble anti-CD28. CFSE profiles are gated on $CD8^+$ cells and the actual number of cells run on the FACS in a fixed period is plotted. *B* and *C*, The cells were analyzed for the surface expression of CD69 and CD25 following stimulation with anti-CD3 in the absence (*B*) or presence (*C*) of anti-CD28. Plots are gated on WT or $Erk2^{T-/-}$ CD8 T cells. The data presented are representative of more than five independent experiments.

In corroboration of the CFSE studies, WT and $Erk2^{T-/-}$ populations possessed a similar proportion of live cells at the different stages of cell cycle at day 2. Furthermore, similar to the results obtained using annexin V, we observed few subdiploid or dead cells (expressed as percentage of total events) at day 2. However, by day 3 there was a 2-fold increase in the subdiploid peak in the $Erk2^{T-/-}$ group when compared with the WT cells at the same time point. The increased death in the $Erk2^{T-/-}$ cells was accompanied by a loss in the proportion of dividing cells, again suggesting that Erk2 promotes survival of proliferating CD8 T cells.

IL-2 is an important growth and survival factor for T cells in vitro (39), and Erk activity is thought to be essential for transcription of the IL-2 gene (40). Hence, we determined whether CD8 T cells were capable of producing IL-2 in the absence of Erk2. We measured IL-2 levels within the culture supernatants or WT and $Erk2^{T-/-}$ CD8 T cells following stimulation with anti-CD3 and anti-CD28. Consistent with previous observations (41), IL-2 production by WT CD8 T cells peaked at early time points postactivation and then declined quite rapidly (Fig. 4*C*). Analyses of the $Erk2^{T-/-}$ cell supernatants revealed a severe defect in IL-2 production at all time points assayed. Previous work has demonstrated that IL-2 is not required for the initiation of cell cycling within CD8 T cells, but it supports their survival at later stages of proliferation (42). We wondered whether the decreased survival exhibited by the $Erk2^{T-/-}$ cells in vitro could be explained solely on the basis of decreased IL-2 production. To test this, IL-2 was added to WT and $Erk2^{T-/-}$ cell cultures during activation, and the numbers of cell divisions and cell viability were measured as before. The addition of IL-2 was capable of rescuing impaired $Erk2^{T-/-}$ cell survival at day 3, but not at a later time point (Fig. 4*D*, *left panels*). Thus, we only observed partial rescue of $Erk2^{T-/-}$ cell survival. Similar results were obtained when the $Erk2^{T-/-}$ CD8 T cells were provided with an identical cytokine milieu as the WT cells by coculturing congenically marked WT and $Erk2^{T-/-}$ cells in the same wells (Fig. 4*D*, *right panels*). Thus, the reduced survival displayed by the $Erk2^{T-/-}$ CD8 T cells at later time points postactivation in vitro cannot be explained strictly on the basis of altered cytokine production and must include a cell-intrinsic defect.

Erk2 is required for activated CD8 T cell survival in vivo

To determine whether we could observe a similar role for Erk2 during immune responses in intact animals, we immunized WT or $Erk2^{T-/-}$ mice with LCMV and sacrificed mice at days 5 and 8 postinfection. Day 5 postinfection was the earliest time point at which it was possible to easily visualize a substantial population of LCMV-specific CD8 T cells using class I tetramers. At this time

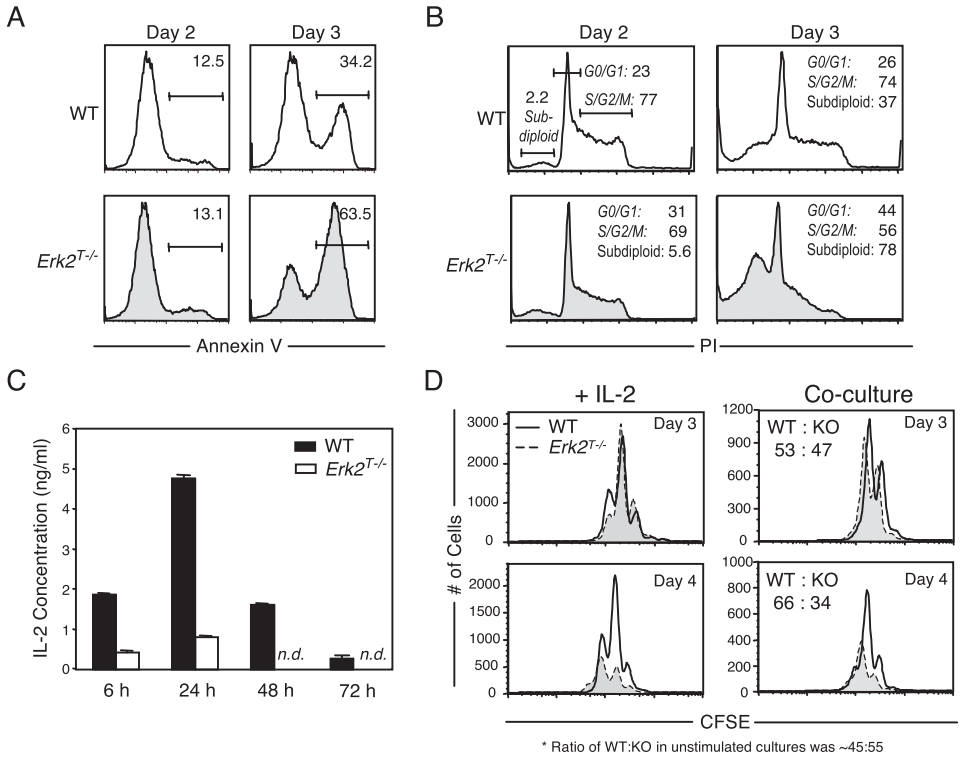

FIGURE 4. Erk2 is critical for activated CD8 T cell survival. *A* and *B*, Purified WT or *Erk2*$^{T-/-}$ CD8 T cells were activated with plate-bound anti-CD3 and soluble anti-CD28, and analyzed by FACS following staining with (*A*) annexin V or (*B*) PI. The annexin V histograms were gated on all events, and numbers indicated are percentage of all events. The PI data were analyzed using ModFit LT software, and the proportion of subdiploid cells is expressed as a percentage of total events, while the proportion of cells at the different stages of cell cycle (G_0/G_1 or $S/G_2/M$) are expressed as a percentage of live events. The data presented are representative of three (for annexin V) and four (for PI) independent experiments. *C*, Purified WT or *Erk2*$^{T-/-}$ CD8 T cells were activated as in *A*, and the levels of IL-2 in culture supernatants were estimated at indicated time points using an ELISA. (n.d. indicates not detected). The data presented are the means ± SD and are representative of two independent experiments. *D*, CFSE-labeled CD45.1$^+$ WT and CD45.2$^+$ *Erk2*$^{T-/-}$ CD8 T cells were activated for indicated time points in the presence of rhIL-2 (*left panel*) or were cocultured in the same wells (*right panel*). CFSE profiles are gated on WT or *Erk2*$^{T-/-}$ CD8$^+$ cells and the actual number of cells run on the FACS in a fixed period is plotted. Also shown in the coculture experiments is the ratio of WT to *Erk2*$^{T-/-}$ cells. This ratio in unstimulated cultures was ~45:55. The data presented are representative of two independent experiments.

point, the *Erk2*$^{T-/-}$ mice had mounted a strong CD8 T cell response to LCMV (Fig. 5*A*, *top panels*), but already appeared to possess slightly reduced proportions and numbers of LCMV-specific CD8 T cells. However, by the peak of the proliferative phase (day 8), there was a dramatic reduction in the proportion as well as the absolute number of NP_{396}-specific CD8 T cells present within the spleens of *Erk2*$^{T-/-}$ mice (Fig. 5*A*, *bottom panels*). The fold expansion for the *Erk2*$^{T-/-}$ NP_{396}-specific CD8 T cell population between day 5 and day 8 was only 6-fold compared with the ~22-fold increase displayed by the WT cells. In contrast to this impressive phenotype that was observed in the absence of Erk2, CD8 T cell responses within secondary lymphoid tissues of mice deficient in IL-2 or CD25 are only marginally impaired (42, 43). This is consistent with the notion that the *Erk2*$^{T-/-}$ phenotype is not merely due to a reduction in IL-2 production. We also confirmed these results by tracking the GP_{33}-specific CD8 T cell response using class I tetramers (data not shown). Thus, following a viral infection in vivo, all responding CD8 T cells displayed considerable dependence on Erk2 for optimal expansion.

Although Erk2 clearly affected the survival but not the extent of cell division following in vitro stimulation, we sought to distinguish between these two aspects of expansion in vivo. We could not assess the proportion of dying cells, presumably due to the rapid engulfment associated with apoptosis; however, we determined the proportion of dividing cells by measuring the incorporation of BrdU into the DNA of dividing cells. Groups of WT and *Erk2*$^{T-/-}$ mice were injected with BrdU at day 4.5 or day 7.5 postinfection. The mice were then sacrificed ~16 h later (i.e., day 5 and day 8), and BrdU incorporation was measured using flow cytometry. The results showed that similar proportions of the WT and *Erk2*$^{T-/-}$ NP_{396}-specific cells had incorporated BrdU during the 16-h labeling period at day 5 (data not shown) as well as on day 8 (Fig. 5*B*). This demonstrated that even during the latter stages of the expansion phase, just before the expansion peak, LCMV-specific *Erk2*$^{T-/-}$ CD8 T cells were synthesizing DNA at a rate that was equivalent to the WT population. We conclude that Erk2 plays an important role in maintaining CD8 T cell survival, but not cell division, during the latter stages of the expansion phase in vivo.

We next examined the functional capacity of the responding CD8 T cells that were generated in the absence of Erk. Quantification of the LCMV-specific CD8 T cell response using intracellular IFN-γ staining (Fig. 5*C*) demonstrated a similar fold decrease of *Erk2*$^{T-/-}$ T cells as had been observed using MHC class I tetramer staining. This result indicated that the responding *Erk2*$^{T-/-}$ NP_{396}-specific cells were proficient at effector cytokine (IFN-γ) production. Measurement of CD8 T cell cytotoxic activity at the peak of the response (day 8) revealed lower CTL activity within *Erk2*$^{T-/-}$ mice (Fig. 5*D*, *left panel*). However, this decrease was due to the reduced numbers of peptide-specific cells within *Erk2*$^{T-/-}$ mice, as we observed no difference in CTL activity after normalizing for the actual number of Ag-specific cells present within each well (Fig. 5*D*, *right panel*). IFN-γ production and CTL

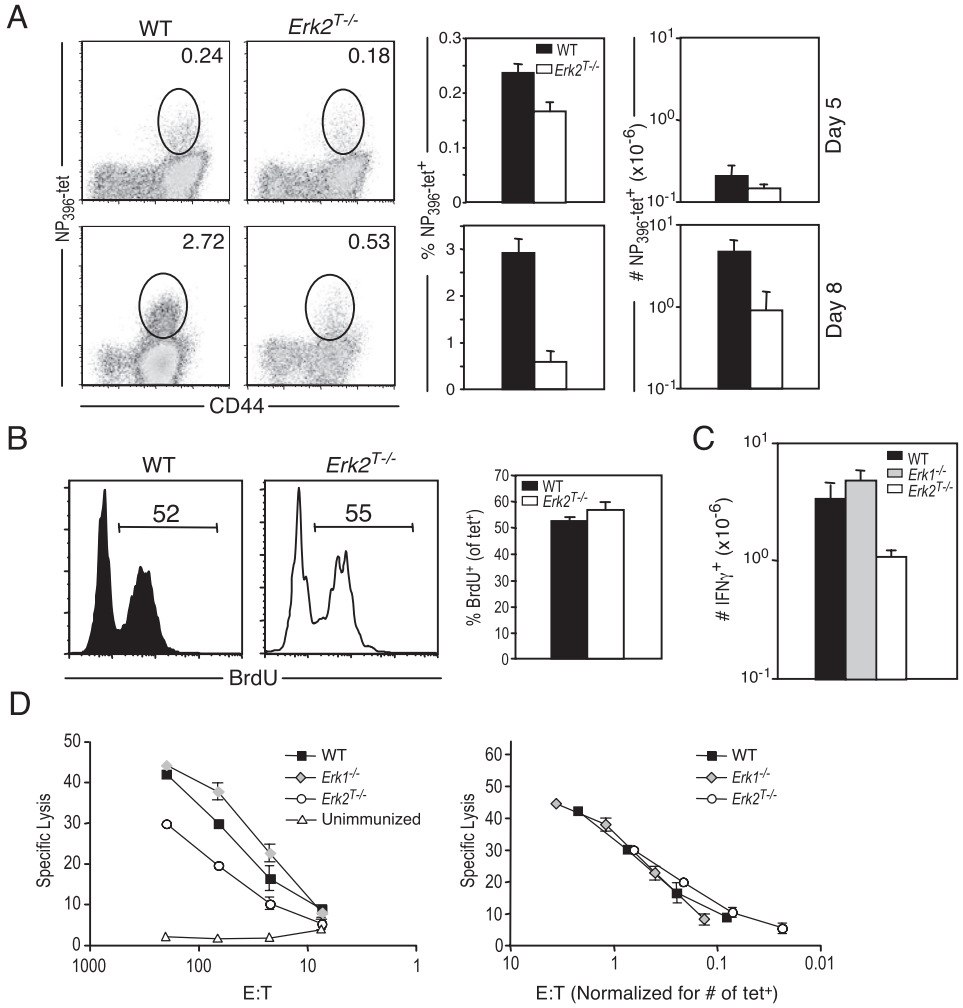

FIGURE 5. Erk2 is requisite for CD8 T cell survival, but not for effector function in vivo. Mice were infected i.p. with 2×10^5 PFU LCMV. Ag-specific CD8 T cell responses within the spleen were assayed at indicated time points postinfection using H-2D^b-NP$_{396}$ tetramers (*A* and *B*) or intracellular IFN-γ staining (*C*). *A*, Representative FACS plots of WT and *Erk2*$^{T-/-}$ mice (gated on CD8$^+$ cells), percentage, and total numbers of Ag-specific cells present in spleen on days 5 and 8 postinfection. The numbers shown in the FACS plots are percentage of total lymphocytes, and the bar graphs depict the means ± SD for a cohort of mice. The data presented are representative of more than five independent experiments. *B*, To determine the proportion of cycling cells late in the expansion phase, mice were injected with BrdU at about day 7.5 and sacrificed 16 h later. Plots are gated on tetramer-positive CD44^{high}CD8$^+$ T cells, and numbers indicate the percentage of gated population that are BrdU-positive. The data presented are representative of two independent experiments. *C*, WT, *Erk1*$^{-/-}$, and *Erk2*$^{T-/-}$ mice were infected with LCMV as in *A*, and splenocytes were isolated at day 8 postinfection and analyzed for intracellular IFN-γ production following short-term restimulation in vitro. The data presented are the means ± SD and are representative of three independent experiments. *D*, CTL activity was measured using the splenocytes from day 8 LCMV-infected WT, *Erk1*$^{-/-}$, and *Erk2*$^{T-/-}$ mice and an unimmunized control. *Left panel*, mean ± SD for one representative mouse from each group is shown; *right panel*, the normalized data based on the actual number of peptide-specific (tetramer-positive) CD8 T cells in each well are plotted. These data are representative of two independent experiments.

activity were also completely normal within *Erk1*$^{-/-}$ mice (Fig. 5*D*), suggesting that CD8 T cells are capable of differentiating into functionally competent effector cells even in the absence of Erk1 or Erk2.

To generalize our conclusions to other CD8 T cell responses in vivo, we infected WT or *Erk2*$^{T-/-}$ mice with VSV and analyzed the responding CD8 T cells using MHC class I tetramers specific for a peptide derived from the VSV nucleocapsid protein (RGYVYQGL). At an early time point (day 4) before the peak of expansion, we observed identical percentages of VSV-specific CD8 T cells in peripheral blood, demonstrating that early expansion in the absence of Erk2 proceeded normally (Fig. 6*A*, *left panel*). Similar to the results obtained using LCMV, by the peak of the anti-VSV response (days 6–7), there were dramatically reduced proportions and numbers of the VSV-specific CD8 T cells in the blood (Fig. 6*A*, *right panel*) and spleens (Fig. 6*B*) of *Erk2*$^{T-/-}$ mice. We note that the requirement for Erk2 in supporting cell survival was only observed during the expansion phase, and not during the contraction phase. In fact, we observed a slightly reduced contraction (when normalized to the peak of expansion) in the absence of Erk2 (Fig. 6*A*, *right panel*) and are currently in the process of determining the relevance of these results. As mentioned earlier, T cells were the only cells that were Erk2-deficient within the conditional knockout *Erk2*$^{T-/-}$ mice. Nonetheless, to ensure that the results that we had obtained were solely due to an Erk2 deficiency within the CD8 T cell compartment, we performed the following set of experiments. We generated TCR transgenic mice on the *Erk2*$^{T-/-}$ background (OT-I$^+$*Erk2*$^{T-/-}$) and adoptively transferred a small number (1000) of WT OT-I$^+$ or OT-I$^+$*Erk2*$^{T-/-}$ cells (CD45.2$^+$) to congenically marked (CD45.1$^+$) naive mice. The mice were immunized a day later with VSV-OVA, and the OVA-specific donor (OT-I$^+$) and

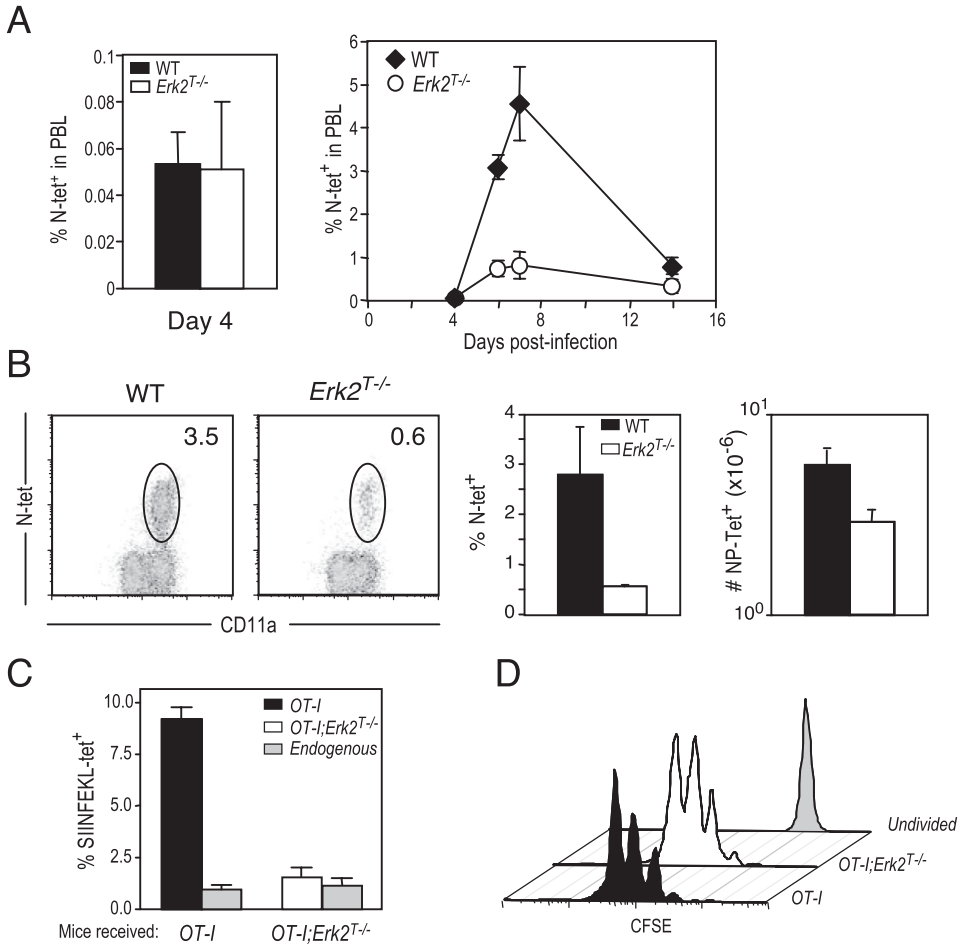

FIGURE 6. Erk2 is required for CD8 T cell survival following infection with VSV. *A*, WT or $Erk2^{T-/-}$ CD8 T cells were infected i.v. with VSV, and Ag-specific CD8 T cell responses in peripheral blood were assayed at indicated time points using H-2K^b-RGYVYQGL tetramers. Percentages of PBL that are tetramer-positive are shown. The data presented are the means ± SD and are representative of two independent experiments. *B*, Representative FACS plots of WT and $Erk2^{T-/-}$ mice (gated on CD8$^+$ cells), percentage, and total numbers of Ag-specific cells present in spleen on day 6 postinfection. The numbers shown in the FACS plots are percentage of total lymphocytes, and the bar graphs depict the mean ± SD for a cohort of mice. The data presented are representative of two independent experiments. *C* and *D*, Congenically marked (CD45.1$^+$) naive mice received an i.v. transfer of 1000 unlabeled (*C*) or 0.5×10^6 CFSE-labeled (*D*) WT or $Erk2^{T-/-}$ OT-I cells 1 day before immunization with VSV-OVA. Spleens were isolated at day 2 (*D*) or day 6 (*C*) postinfection and analyzed by FACS for the presence of OVA-specific donor (OT-I) and host (endogenous) CD8 T cells. The graphs presented in *C* are expressed as a percentage of total lymphocytes in the spleen, and the plots in *D* are gated on donor OT-I cells (CD45.2$^+$CD8$^+$). Also indicated in *D* are the levels of CFSE within undivided cells. The data are representative of two independent experiments.

endogenous (control) populations at the peak of the response (day 6) were visualized using the congenic marker and class I tetramers, respectively (Fig. 6*C*). Consistent with all of our earlier results, we again observed diminished accumulation of the OT-I$^+$$Erk2^{T-/-}$ cells at the peak of the response compared with the WT OT-I cells. As expected, the size of the control (endogenous) responding population in both groups of mice was similar. We also confirmed our conclusion that cell division proceeds normally in the absence of Erk2 by transferring a higher number (0.5×10^6) of CFSE-labeled WT or $Erk2^{T-/-}$ OT-I cells and analyzing their division profiles at 48 h postinfection with VSV-OVA (Fig. 6*D*).

Erk2 regulates expression of the Bcl-2 family of proteins

Since the in vivo results mirrored our in vitro observations, we made use of the in vitro system to delineate the molecular pathways downstream of Erk2 that enhanced CD8 T cell survival. We performed microarray analyses on RNA isolated from WT and $Erk2^{T-/-}$ cells that had been stimulated with anti-CD3 and anti-CD28 for 2 days. We chose the day 2 time point because this was the last time point at which the viability and proliferation of WT and $Erk2^{T-/-}$ CD8 T cells were identical (Fig. 3*A*). As mentioned above, the Bcl-2 members Bcl-2, Bcl-x_L, and Bim are thought to be the key regulators of T cell survival, and microarray analyses from two independent experiments revealed reduced expression of the prosurvival members (Bcl-2 and Bcl-x) and increased levels of the proapoptotic member (Bim) within the $Erk2^{T-/-}$ CD8 T cells when compared with the WT controls (Fig. 7*A*). Importantly, these differences were not observed within similarly stimulated $Erk1^{-/-}$ CD8 T cells, indicating that this alteration in gene expression was specific to Erk2. Furthermore, no such changes were observed within the $Erk2^{T-/-}$ CD8 T cells before stimulation (Fig. 7*A*).

We then used quantitative real-time PCR to measure the levels of Bcl-2, Bcl-x_L, and the three isoforms of Bim in the day 2 activated WT and $Erk2^{T-/-}$ CD8 T cells. Consistent with our microarray studies, we observed reduced levels of Bcl-2 and Bcl-x_L, along with increased levels of Bim within the $Erk2^{T-/-}$ cells (Fig. 7*B*). We next determined whether the observed alterations in gene expression were also manifest at the protein level. To this end, WT

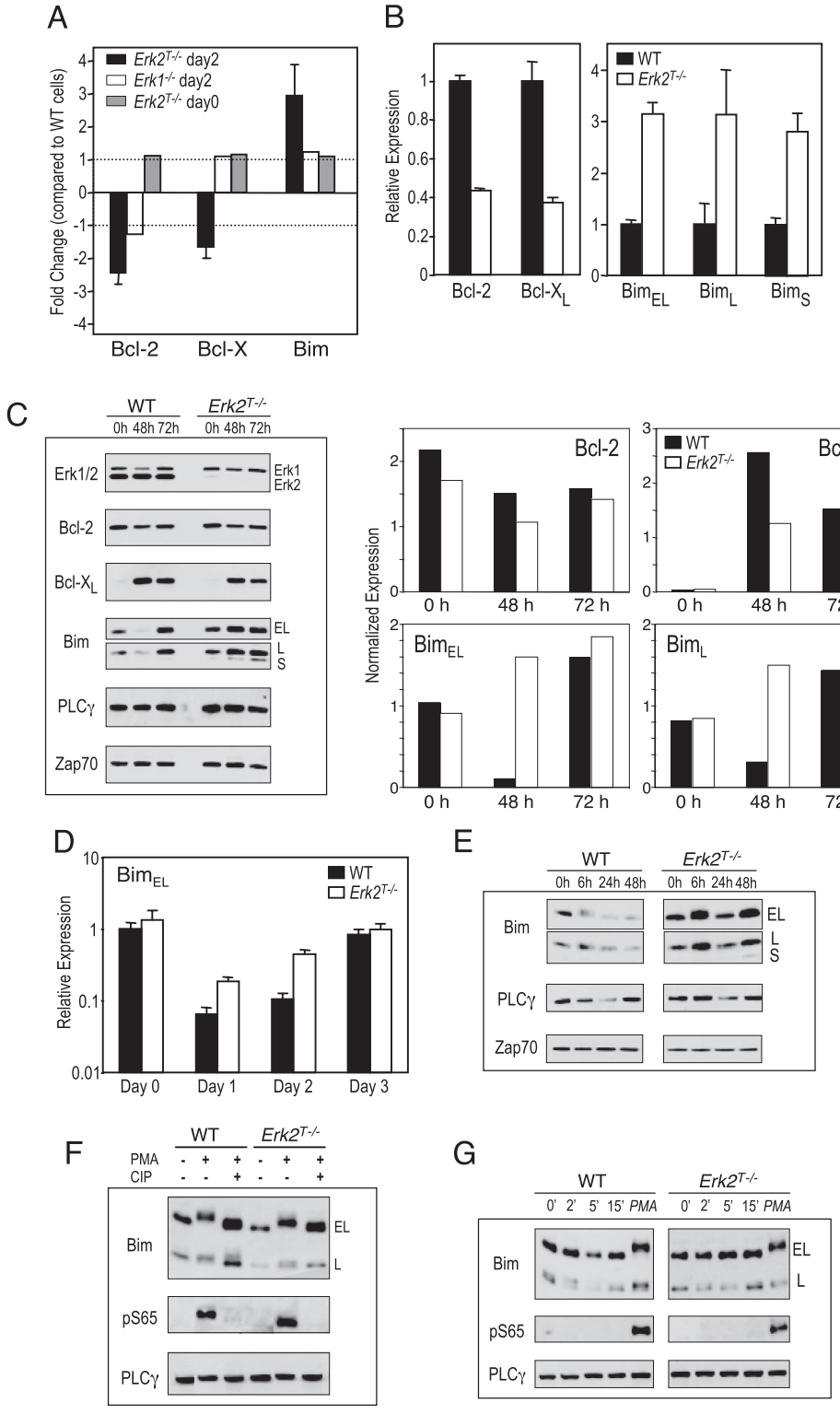

FIGURE 7. Erk2 regulates the expression of Bcl-2 family members. *A*, RNA was isolated from unstimulated WT and $Erk2^{T-/-}$ CD8 T cells or WT, $Erk1^{-/-}$, or $Erk2^{T-/-}$ CD8 T cells that had been stimulated for 2 days with plate-bound anti-CD3 and soluble anti-CD28. Gene arrays were performed and the levels of Bcl-2, Bcl-x, and Bim present in the Erk-deficient cell types are expressed as a fold change in gene expression compared with that in the WT controls. Thus, positive and negative values indicate up-regulation and down-regulation, respectively, within the Erk-deficient cells. The data plotted are the means ± SE of two independent experiments comparing the day 2 stimulated WT and $Erk2^{T-/-}$ cells, and one experiment each for the other two sets. *B* and *D*, The mRNA levels of the indicated genes were measured at day 2 (*B*) or indicated time points (*D*) postactivation using real-time quantitative PCR. Following normalization to a housekeeping gene, the levels of gene expression cells were further normalized to the respective WT control (*B*) or to the day 0 WT sample (*D*). *C* and *E*, Purified CD8 T cells from WT or $Erk2^{T-/-}$ mice were stimulated in vitro with plate-bound anti-CD3 and soluble anti-CD28. Cell lysates were analyzed by Western blotting for the indicated proteins at various time points following activation. Zap-70 and PLCγ were used as loading controls. Also plotted are protein levels after normalization to PLCγ. *F*, Purified CD8 T cells from WT or $Erk2^{T-/-}$ mice were stimulated for 15 min with PMA, and cell lysates were treated (or not) with calf intestinal phosphatase and analyzed by Western blotting. *G*, Same as Fig. 6*C*, along with the addition of PMA-stimulated cell lysates (15 min) as a positive control.

and $Erk2^{T-/-}$ CD8 T cells were activated with anti-CD3 and anti-CD28, harvested at days 2 and 3 postactivation, and cell lysates were probed for Erk1/2, Bcl-2, Bcl-x_L, and Bim by Western blotting (Fig. 7*B*). PLCγ and Zap70 were used as loading controls. As expected, upon blotting for Erk1 and Erk2, we did not observe any Erk2 protein in the $Erk2^{T-/-}$ cells at all time points. This result demonstrated that the normal proliferation that was observed in the absence of Erk2 was not due to a few cells that may not have deleted the *Erk2* gene. A comparison of Bcl-2 levels within activated WT and $Erk2^{T-/-}$ CD8 T cell lysates revealed variable results wherein the levels of Bcl-2 present within the $Erk2^{T-/-}$ cells were decreased to a greater extent in some (data not shown) but not all experiments (Fig. 7*C*). In contrast, we consistently observed reduced induction of Bcl-x_L within $Erk2^{T-/-}$ cells, and the most striking result was obtained when we examined the levels of the proapoptotic molecule Bim. Based on the current understanding of Bim regulation in T cells and our experiments measuring Bim transcripts, we expected Bim levels within activated WT CD8 T cells to remain unaltered but to be up-regulated within the $Erk2^{T-/-}$ cells. To our surprise, we observed that Bim levels were

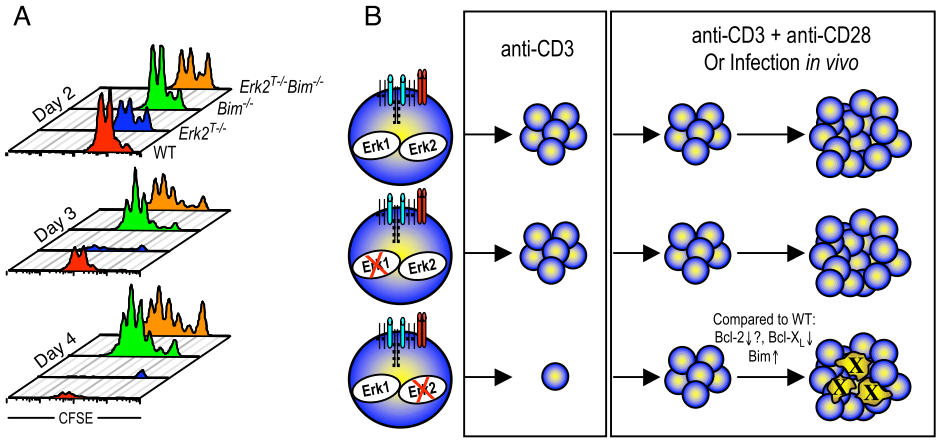

FIGURE 8. Rescue of Erk2-deficient CD8 T cell survival by Bim deficiency. *A*, Purified CD8 T cells from WT, *Erk2*$^{T-/-}$, *Bim*$^{-/-}$, and *Erk2*$^{T-/-}$*Bim*$^{-/-}$ mice were stimulated in vitro for indicated periods with plate-bound anti-CD3 and soluble anti-CD28. CFSE profiles are gated on CD8$^+$ cells, and the actual number of cells run on the FACS in a fixed period is plotted. The data presented are representative of two independent experiments. *B*, A model depicting the effect of deletion of either Erk1 or Erk2 on CD8 T cell proliferation and survival following activation with anti-CD3 alone, anti-CD3 + anti-CD28, or a viral infection in vivo.

reduced in WT CD8 T cells at 48 h postactivation but resumed higher levels by 72 h (Fig. 7*C*). In contrast, *Erk2*$^{T-/-}$ CD8 T cells maintained high levels of Bim throughout. Additionally, the levels of Bim were also higher within *Erk2*$^{T-/-}$ CD8 T cells that had been activated for 2 days in the presence of IL-2, as compared with the WT controls (data not shown).

Analyses of Bim$_{EL}$ transcripts at different time points postactivation revealed a dramatic down-regulation of Bim expression following stimulation of WT CD8 T cells (Fig. 7*D*). Interestingly, Bim levels were also down-regulated within the *Erk2*$^{T-/-}$ cells at 24 h poststimulation, albeit not to the same level as that observed within the WT cells. Furthermore, at 48 h poststimulation, the *Erk2*$^{T-/-}$ cells contained far greater levels of Bim$_{EL}$ transcripts (Fig. 7*D*). Similar results were obtained on measuring the levels of Bim$_L$ and Bim$_S$ transcripts (data not shown) and demonstrated that an important facet of Erk2 signaling is the inhibition of Bim expression in activated T cells.

The accelerated kinetics of Bim transcript up-regulation observed in the activated *Erk2*$^{T-/-}$ CD8 T cells are consistent with studies demonstrating a role for Erk in fibroblast and epithelial cell survival by preventing de novo Bim reexpression following the withdrawal of survival factors (44, 45). However, others have also demonstrated that Erk-mediated phosphorylation of Bim$_{EL}$ and perhaps Bim$_L$ leads to their ubiquitination and degradation (44, 46). In light of these studies, we wanted to investigate the Erk2-dependent posttranslational regulation of Bim. We assayed Bim levels at earlier time points postactivation with anti-CD3 and anti-CD28, and observed Bim down-regulation within WT, but not *Erk2*$^{T-/-}$, cells (Fig. 7*E*). Phosphorylation of Bim$_{EL}$ following PMA stimulation of thymocytes and splenocytes has been shown to result in a marked retardation of mobility on SDS-PAGE gels (47), and while we did observe a Bim$_{EL}$ band of slightly reduced mobility at 6 h poststimulation of WT and *Erk2*$^{T-/-}$ cells with anti-CD3 and anti-CD28 (Fig. 7*E*), the mobility shift was marginal. Furthermore, treatment of the lysates with a phosphatase did not alter this shift, and the use of Abs that recognize the Erk-phosphorylated Ser^{65} residue of Bim (46) yielded negative results (data not shown).

As a positive control we stimulated WT CD8 T cells with PMA and observed a Bim$_{EL}$ band of reduced mobility (Fig. 7*F*) that was not present in phosphatase-treated cell lysates. This indicated that the shifted band corresponded to a phosphorylated form of Bim$_{EL}$, and we confirmed this result by blotting with the anti-pS65 Ab (Fig. 7*F*). However, this phosphorylated band was also present in the PMA-stimulated *Erk2*$^{T-/-}$ cells, suggesting that PMA stimulation led to the Erk2-independent phosphorylation of S65. We next examined Bim phosphorylation at 2, 5, or 15 min following anti-CD3 and anti-CD28 stimulation and failed to observe Bim$_{EL}$ phosphorylation at any time point, as judged by a lack of mobility shift and the absence of a band following blotting with anti-Bim or anti-pS65, respectively (Fig. 7*G*). We also did not observe Bim$_{EL}$ phosphorylation in either WT or *Erk2*$^{T-/-}$ cells following stimulation with a 100-fold higher concentration of anti-CD3 in the presence of anti-CD28 (data not shown). In summary, we were unable to detect Erk2-dependent posttranslational regulation of Bim even following superoptimal stimulation of CD8 T cells with anti-CD3 and anti-CD28. Importantly, we did observe a critical role for Erk2 in inhibiting the expression of Bim transcripts under these conditions.

Rescue of impaired Erk2$^{T-/-}$ *CD8 T cell survival by Bim deficiency*

As described above, the ratio of Bcl-2 and Bcl-x$_L$ to that of the proapoptotic member Bim appears to regulate T cell survival and death. Our results indicate that Erk2-mediated regulation of these key Bcl-2 family members led to a ratio in favor of the proapoptotic molecule Bim in the absence of Erk2. To determine whether it was possible to shift this balance and thus rescue the survival defect observed in *Erk2*$^{T-/-}$ CD8 T cells, we generated mice that were deficient for both Erk2 and Bim (*Erk2*$^{f/f}$*dLck-icre*$^+$*Bim*$^{-/-}$). CFSE-labeled CD8 T cells from *Erk2*$^{T-/-}$, *Bim*$^{-/-}$, and *Erk2*$^{T-/-}$ *Bim*$^{-/-}$ littermates were either left unstimulated or were stimulated with anti-CD3 and anti-CD28 in vitro. A nonlittermate B6 mouse was also included as a WT control. When left unstimulated, both *Bim*$^{-/-}$ and *Erk2*$^{T-/-}$*Bim*$^{-/-}$ CD8 T cells displayed an impressive survival advantage (data not shown) consistent with a role for Bim in promoting naive T cell survival (30). Upon stimulation with anti-CD3 and anti-CD28, we observed a slight reduction in proliferation of the *Erk2*$^{T-/-}$ and *Erk2*$^{T-/-}$*Bim*$^{-/-}$ cells on day 2 (Fig. 8*A*, *top panel*) that appears to be related to their mixed genetic background. However, at days 3 and 4 (Fig. 8*A*, *middle* and *bottom panels*), consistent with our previous observations, survival of proliferating *Erk2*$^{T-/-}$ cells was greatly impaired. As expected, the *Bim*$^{-/-}$ cells displayed a survival advantage compared with the WT cells, but, more importantly, the *Erk2*$^{T-/-}$*Bim*$^{-/-}$ cell population displayed proliferative and survival characteristics not substantially different from *Bim*$^{-/-}$ cells. These data show that in the absence of Bim, Erk2 is dispensable for T cell survival and expansion, and they support the hypothesis that Erk2 regulates the survival of proliferating CD8 T cells, at least in part, by regulating the ratio of proapoptotic and prosurvival Bcl-2 family members.

Discussion

The factors driving T cell activation and expansion are several and include both positive and negative regulators. As a result, the cell fate decisions made by activated T cells are the outcome of an integration of signals originating from a variety of different signaling cascades. In this report, we have demonstrated that Erk2 plays a key role in regulating the expansion phase of T cell responses (Fig. 8*B*). Consistent with the extensive literature pointing to an indispensable role for Erk in cell cycle entry (24, 25), we observed that Erk2 was essential for CD8 T cell proliferation following stimulation of the TCR alone. In contrast, we found that the provision of a costimulatory signal obviated the need for Erk2 in initiating cell cycle progression. These results were confirmed by assaying Ag-specific CD8 T cell responses to different viral pathogens in vivo. Given that Erk1 and Erk2 appear similar in most aspects, the presence of Erk1 might be sufficient to drive cell division under these conditions. However, we observed no defect in $Erk1^{-/-}$ CD8 T cell proliferation even in the absence of costimulation. There are two potential explanations for the preferential dependence of CD8 T cells on Erk2. The first is that this is a consequence of differences in the expression levels of Erk1 and Erk2, with Erk2 being expressed at much higher levels (14). The alternative explanation is that there exist functional differences between these two Erk isoforms (13), as has been reported for the Jnk1 and Jnk2 MAPK isoforms during CD8 T cell responses (48, 49).

As mentioned above, CD8 T cells that were activated in the absence of Erk2 using anti-CD3 and anti-CD28 proliferated normally, but under these conditions Erk2 delivered an indispensable survival signal to the proliferating cells (Fig. 8*B*). Our preliminary studies analyzing $Erk1^{+/-}Erk2T^{-/-}$ CD8 T cells indicate that survival of these cells is impaired to a greater degree than in the absence of Erk2 alone (our unpublished observations). This suggests that the functions of Erk1 overlap those of Erk2, and that the extent of Erk signaling is a determining factor in the size of the T cell expansion in response to pathogen challenge. An important T cell growth and survival factor is IL-2, and we observed that the $Erk2^{T-/-}$ cells displayed greatly impaired production of IL-2 at all time points examined. This finding is likely due to the fact that Erk is thought to be required for the expression of Fos family members, formation and stabilization of AP-1 complexes, and subsequent IL-2 production (40, 50). In support of this conclusion, we observed dramatically reduced levels of c-Fos, Fra-1, and Fra-2 in the absence of Erk2 (our unpublished observations). Despite this fact, we noticed no difference in the ability of the $Erk2^{T-/-}$ cells to proliferate normally, consistent with studies demonstrating that IL-2 is not required for the initiation of CD8 T cell proliferation (42). However, in contrast to the relatively normal CD8 T cell responses that are observed within secondary lymphoid tissues of mice deficient in IL-2 or CD25 (42, 43, 51), $Erk2^{-/-}$ mice exhibited greatly impaired primary CD8 T cell responses in vivo. These data strongly suggest that the diminished survival exhibited by CD8 T cells in the absence of Erk2 could not be explained solely on the basis of a reduction in IL-2 production. Consistent with this conclusion, we only observed partial rescue of $Erk2^{T-/-}$ CD8 T cell survival following the provision of exogenous IL-2 or following coculture with WT CD8 T cells.

It has been demonstrated that the programming of CD8 T cell expansion during the priming phase allows for extended proliferation even after removal of the activating stimuli (52–54). We demonstrated that survival, not cell division, was impaired in the absence of Erk2, and the simplest explanation is that continued Erk signaling determines the extent of T cell expansion. However, it is possible that the level of Erk2 signaling during the priming phase programs the subsequent survival rate, and we are currently developing the tools to address this issue.

We note that other molecules implicated as upstream or downstream members of the Erk cascade appear to play an analogous role in supporting CD8 T cell survival. For example, in marked similarity to our results, Altman and colleagues have suggested that PKCθ-dependent activation of Erk and Jnk promotes in vitro-activated CD8 T cell survival by negatively regulating Bim_{EL} (55). However, reports that CD8 T cell responses to different viral infections in vivo proceed normally in the absence of PKCθ (56) suggests that other signals overcome the requirement for PKCθ for optimal MAPK activation in vivo. The Ras-guanyl nucleotide exchange factor RasGRP1 is an important constituent of the TCR signaling machinery that leads to the activation of the Ras-Erk cascade (57). As a result, RasGRP1-null CD8 T cells undergo normal early activation events in response to Ag, but fail to sustain proliferation (58). Id proteins (Id1–Id4) are a group of proteins that alter gene expression by inhibiting the activity of the E-box protein transcription factors (59). The Ras-Erk cascade has been shown to lead to the induction of Id proteins such as Id3 in thymocytes (60), and CD8 T cells deficient in Id2 display a survival defect that mirrors that seen in the $Erk2^{T-/-}$ CD8 T cells (61). Although these observations suggested that the Erk2-driven survival signal might proceed via Id2, our preliminary results revealed no significant differences in the levels of Id2 in the activated WT and $Erk2^{T-/-}$ cells (our unpublished observations).

The current notion that Bim levels within activated T cells remain unchanged is based primarily on studies investigating Bim levels at the peak of the expansion phase (30). We also confirmed that Bim is expressed at high levels at later time points postactivation but obtained the unexpected finding that Bim levels are dramatically down-regulated in WT CD8 T cells at early time points postactivation. Similar observations were made by Sabbagh et al. upon measuring the levels of Bim in activated OT-I CD8 T cells (62). Thus, although apoptosis occurring during the contraction phase is likely the result of reduced levels of the antiapoptotic molecules as has been suggested, we have now provided evidence that the transcriptional down-regulation of proapoptotic molecule Bim regulates CD8 T cell survival during the expansion phase. Consistent with this hypothesis are the observations that the withdrawal of survival factors from other cell types can lead to the expression of Bim and apoptosis (44). Importantly, in fibroblasts, the activation of Erk during serum withdrawal correlated with reduced Bim levels, whereas inhibition of Erk signaling led to an increase in Bim message (45). The question then arises as to the mechanism of Erk-mediated regulation of Bim transcription. It has been demonstrated that the withdrawal of cytokines leads to the activation of the forkhead box O transcription factor FoxO3 (FKHRL1), which then directly up-regulates Bim transcription (63). It has also been reported that Erk regulates FoxO1 activity by phosphorylation (64), and very recent work has demonstrated a direct role for Erk in the phosphorylation and degradation of FoxO3 (65). Thus, it is tempting to speculate that Erk regulates Bim transcription via the FoxO transcription factors. In addition to a role for Erk in the regulation of Bim transcription, it has been demonstrated that growth factor stimulation of various cell types leads to an Erk-mediated posttranslational regulation of Bim (44). However, we were unable to visualize Bim phosphorylation following stimulation of WT peripheral CD8 T cells with anti-CD3 and anti-CD28 and observed no requirement for Erk2 in the phosphorylation of Bim that occurred following stimulation with PMA. These data indicate that the levels of Bim in CD8 T cells are not

substantially reduced by posttranslational modifications mediated specifically by Erk2.

The activation of the Erk MAPK is a focal point of signaling in most cell types, and it is interesting to note that >150 molecules have already been identified as putative Erk substrates (7). As a result, it might be expected that Erk can mediate cell fate decisions via several different mediators, only a handful of which we have identified herein. Experiments are underway to identify other potential pathways downstream of Erk within activated T cells and to determine the extent to which it might be possible to manipulate these signals in vivo. Such studies will greatly enhance the development of novel strategies aimed at enhancing or inhibiting CD8 T cell responses in a therapeutic setting.

Acknowledgments

We thank Dr. N. Killeen for providing us with dLck-icre mice; Drs. D. Masopust and V. Vezys for MHC class I tetramers; Drs. D. Hildeman, H. Harada, F. Luciano, and L. Sabbagh for Abs and/or technical advice for studies examining Bim regulation; N. Lind for technical assistance with real-time quantitative PCR; Dr. R. Sasik and J. Lapira for the gene array studies; Dr. E. Zuniga for help with plaque assays; and Drs. K. Beck, C. Murre, and A. Goldrath for critical reading of the manuscript.

Disclosures

The authors have no financial conflicts of interest.

References

1. Murali-Krishna, K., J. D. Altman, M. Suresh, D. J. Sourdive, A. J. Zajac, J. D. Miller, J. Slansky, and R. Ahmed. 1998. Counting antigen-specific CD8 T cells: a reevaluation of bystander activation during viral infection. *Immunity* 8: 177–187.
2. Butz, E. A., and M. J. Bevan. 1998. Massive expansion of antigen-specific $CD8^+$ T cells during an acute virus infection. *Immunity* 8: 167–175.
3. Kaech, S. M., and E. J. Wherry. 2007. Heterogeneity and cell-fate decisions in effector and memory $CD8^+$ T cell differentiation during viral infection. *Immunity* 27: 393–405.
4. Dong, C., R. J. Davis, and R. A. Flavell. 2002. MAP kinases in the immune response. *Annu. Rev. Immunol.* 20: 55–72.
5. Cobb, M. H., T. G. Boulton, and D. J. Robbins. 1991. Extracellular signal-regulated kinases: ERKs in progress. *Cell Regul.* 2: 965–978.
6. Chang, L., and M. Karin. 2001. Mammalian MAP kinase signalling cascades. *Nature* 410: 37–40.
7. Yoon, S., and R. Seger. 2006. The extracellular signal-regulated kinase: multiple substrates regulate diverse cellular functions. *Growth Factors* 24: 21–44.
8. Pages, G., S. Guerin, D. Grall, F. Bonino, A. Smith, F. Anjuere, P. Auberger, and J. Pouyssegur. 1999. Defective thymocyte maturation in p44 MAP kinase (Erk 1) knockout mice. *Science* 286: 1374–1377.
9. Fischer, A. M., C. D. Katayama, G. Pages, J. Pouyssegur, and S. M. Hedrick. 2005. The role of Erk1 and Erk2 in multiple stages of T cell development. *Immunity* 23: 431–443.
10. Yao, Y., W. Li, J. Wu, U. A. Germann, M. S. Su, K. Kuida, and D. M. Boucher. 2003. Extracellular signal-regulated kinase 2 is necessary for mesoderm differentiation. *Proc. Natl. Acad. Sci. USA* 100: 12759–12764.
11. Hatano, N., Y. Mori, M. Oh-hora, A. Kosugi, T. Fujikawa, N. Nakai, H. Niwa, J. Miyazaki, T. Hamaoka, and M. Ogata. 2003. Essential role for ERK2 mitogen-activated protein kinase in placental development. *Genes Cells* 8: 847–856.
12. Saba-El-Leil, M. K., F. D. Vella, B. Vernay, L. Voisin, L. Chen, N. Labrecque, S. L. Ang, and S. Meloche. 2003. An essential function of the mitogen-activated protein kinase Erk2 in mouse trophoblast development. *EMBO Rep.* 4: 964–968.
13. Vantaggiato, C., I. Formentini, A. Bondanza, C. Bonini, L. Naldini, and R. Brambilla. 2006. ERK1 and ERK2 mitogen-activated protein kinases affect Ras-dependent cell signaling differentially. *J. Biol.* 5: 14.
14. Lefloch, R., J. Pouyssegur, and P. Lenormand. 2008. Single and combined silencing of ERK1 and ERK2 reveals their positive contribution to growth signaling depending on their expression levels. *Mol. Cell. Biol.* 28: 511–527.
15. Alberola-Ila, J., and G. Hernandez-Hoyos. 2003. The Ras/MAPK cascade and the control of positive selection. *Immunol. Rev.* 191: 79–96.
16. Mor, A., and M. R. Philips. 2006. Compartmentalized Ras/MAPK signaling. *Annu. Rev. Immunol.* 24: 771–800.
17. Sugawara, T., T. Moriguchi, E. Nishida, and Y. Takahama. 1998. Differential roles of ERK and p38 MAP kinase pathways in positive and negative selection of T lymphocytes. *Immunity* 9: 565–574.
18. Shao, H., E. M. Rubin, L. Y. Chen, and J. Kaye. 1997. A role for Ras signaling in coreceptor regulation during differentiation of a double-positive thymocyte cell line. *J. Immunol.* 159: 5773–5776.
19. Swan, K. A., J. Alberola-Ila, J. A. Gross, M. W. Appleby, K. A. Forbush, J. F. Thomas, and R. M. Perlmutter. 1995. Involvement of p21ras distinguishes positive and negative selection in thymocytes. *EMBO J.* 14: 276–285.
20. Alberola-Ila, J., K. A. Hogquist, K. A. Swan, M. J. Bevan, and R. M. Perlmutter. 1996. Positive and negative selection invoke distinct signaling pathways. *J. Exp. Med.* 184: 9–18.
21. O'Shea, C. C., T. Crompton, I. R. Rosewell, A. C. Hayday, and M. J. Owen. 1996. Raf regulates positive selection. *Eur. J. Immunol.* 26: 2350–2355.
22. Alberola-Ila, J., K. A. Forbush, R. Seger, E. G. Krebs, and R. M. Perlmutter. 1995. Selective requirement for MAP kinase activation in thymocyte differentiation. *Nature* 373: 620–623.
23. Nekrasova, T., C. Shive, Y. Gao, K. Kawamura, R. Guardia, G. Landreth, and T. G. Forsthuber. 2005. ERK1-deficient mice show normal T cell effector function and are highly susceptible to experimental autoimmune encephalomyelitis. *J. Immunol.* 175: 2374–2380.
24. Ashwell, J. D. 2006. The many paths to p38 mitogen-activated protein kinase activation in the immune system. *Nat. Rev. Immunol.* 6: 532–540.
25. Meloche, S., and J. Pouyssegur. 2007. The ERK1/2 mitogen-activated protein kinase pathway as a master regulator of the G1- to S-phase transition. *Oncogene* 26: 3227–3239.
26. DeSilva, D. R., E. A. Jones, M. F. Favata, B. D. Jaffee, R. L. Magolda, J. M. Trzaskos, and P. A. Scherle. 1998. Inhibition of mitogen-activated protein kinase kinase blocks T cell proliferation but does not induce or prevent anergy. *J. Immunol.* 160: 4175–4181.
27. Sharp, L. L., D. A. Schwarz, C. M. Bott, C. J. Marshall, and S. M. Hedrick. 1997. The influence of the MAPK pathway on T cell lineage commitment. *Immunity* 7: 609–618.
28. Agrawal, A., S. Dillon, T. L. Denning, and B. Pulendran. 2006. $ERK1^{-/-}$ mice exhibit Th1 cell polarization and increased susceptibility to experimental autoimmune encephalomyelitis. *J. Immunol.* 176: 5788–5796.
29. Strasser, A., and M. Pellegrini. 2004. T-lymphocyte death during shutdown of an immune response. *Trends Immunol.* 25: 610–615.
30. Marrack, P., and J. Kappler. 2004. Control of T cell viability. *Annu. Rev. Immunol.* 22: 765–787.
31. Strasser, A. 2005. The role of BH3-only proteins in the immune system. *Nat. Rev. Immunol.* 5: 189–200.
32. Pellegrini, M., G. Belz, P. Bouillet, and A. Strasser. 2003. Shutdown of an acute T cell immune response to viral infection is mediated by the proapoptotic Bcl-2 homology 3-only protein Bim. *Proc. Natl. Acad. Sci. USA* 100: 14175–14180.
33. Wojciechowski, S., M. B. Jordan, Y. Zhu, J. White, A. J. Zajac, and D. A. Hildeman. 2006. Bim mediates apoptosis of $CD127^{lo}$ effector T cells and limits T cell memory. *Eur. J. Immunol.* 36: 1694–1706.
34. Hildeman, D. A., Y. Zhu, T. C. Mitchell, P. Bouillet, A. Strasser, J. Kappler, and P. Marrack. 2002. Activated T cell death in vivo mediated by proapoptotic bcl-2 family member bim. *Immunity* 16: 759–767.
35. Puthalakath, H., D. C. Huang, L. A. O'Reilly, S. M. King, and A. Strasser. 1999. The proapoptotic activity of the Bcl-2 family member Bim is regulated by interaction with the dynein motor complex. *Mol. Cell.* 3: 287–296.
36. Zhu, Y., B. J. Swanson, M. Wang, D. A. Hildeman, B. C. Schaefer, X. Liu, H. Suzuki, K. Mihara, J. Kappler, and P. Marrack. 2004. Constitutive association of the proapoptotic protein Bim with Bcl-2-related proteins on mitochondria in T cells. *Proc. Natl. Acad. Sci. USA* 101: 7681–7686.
37. Sandalova, E., C. H. Wei, M. G. Masucci, and V. Levitsky. 2004. Regulation of expression of Bcl-2 protein family member Bim by T cell receptor triggering. *Proc. Natl. Acad. Sci. USA* 101: 3011–3016.
38. Zhang, D. J., Q. Wang, J. Wei, G. Baimukanova, F. Buchholz, A. F. Stewart, X. Mao, and N. Killeen. 2005. Selective expression of the Cre recombinase in late-stage thymocytes using the distal promoter of the Lck gene. *J. Immunol.* 174: 6725–6731.
39. Smith, K. A. 1988. Interleukin-2: inception, impact, and implications. *Science* 240: 1169–1176.
40. Schwartz, R. H. 1997. T cell clonal anergy. *Curr. Opin. Immunol.* 9: 351–357.
41. D'Souza, W. N., and L. Lefrançois. 2004. Frontline: an in-depth evaluation of the production of IL-2 by antigen-specific CD8 T cells in vivo. *Eur. J. Immunol.* 34: 2977–2985.
42. D'Souza, W. N., and L. Lefrançois. 2003. IL-2 is not required for the initiation of CD8 T cell cycling but sustains expansion. *J. Immunol.* 171: 5727–5735.
43. D'Souza, W. N., K. S. Schluns, D. Masopust, and L. Lefrançois. 2002. Essential role for IL-2 in the regulation of antiviral extralymphoid CD8 T cell responses. *J. Immunol.* 168: 5566–5572.
44. Ley, R., K. E. Ewings, K. Hadfield, and S. J. Cook. 2005. Regulatory phosphorylation of Bim: sorting out the ERK from the JNK. *Cell Death Differ.* 12: 1008–1014.
45. Weston, C. R., K. Balmanno, C. Chalmers, K. Hadfield, S. A. Molton, R. Ley, E. F. Wagner, and S. J. Cook. 2003. Activation of ERK1/2 by ΔRaf-1:ER* represses Bim expression independently of the JNK or PI3K pathways. *Oncogene* 22: 1281–1293.
46. Harada, H., B. Quearry, A. Ruiz-Vela, and S. J. Korsmeyer. 2004. Survival factor-induced extracellular signal-regulated kinase phosphorylates BIM, inhibiting its association with BAX and proapoptotic activity. *Proc. Natl. Acad. Sci. USA* 101: 15313–15317.
47. Luciano, F., A. Jacquel, P. Colosetti, M. Herrant, S. Cagnol, G. Pages, and P. Auberger. 2003. Phosphorylation of Bim-EL by Erk1/2 on serine 69 promotes its degradation via the proteasome pathway and regulates its proapoptotic function. *Oncogene* 22: 6785–6793.
48. Conze, D., T. Krahl, N. Kennedy, L. Weiss, J. Lumsden, P. Hess, R. A. Flavell, G. Le Gros, R. J. Davis, and M. Rincon. 2002. c-Jun NH_2-terminal kinase (JNK)1 and JNK2 have distinct roles in $CD8^+$ T cell activation. *J. Exp. Med.* 195: 811–823.

49. Arbour, N., D. Naniche, D. Homann, R. J. Davis, R. A. Flavell, and M. B. Oldstone. 2002. c-Jun NH_2-terminal kinase (JNK)1 and JNK2 signaling pathways have divergent roles in $CD8^+$ T cell-mediated antiviral immunity. *J. Exp. Med.* 195: 801–810.
50. Whitmarsh, A. J. 2007. Regulation of gene transcription by mitogen-activated protein kinase signaling pathways. *Biochim. Biophys. Acta* 1773: 1285–1298.
51. Williams, M. A., A. J. Tyznik, and M. J. Bevan. 2006. Interleukin-2 signals during priming are required for secondary expansion of $CD8^+$ memory T cells. *Nature* 441: 890–893.
52. Wong, P., and E. G. Pamer. 2001. Cutting edge: Antigen-independent CD8 T cell proliferation. *J. Immunol.* 166: 5864–5868.
53. van Stipdonk, M. J., E. E. Lemmens, and S. P. Schoenberger. 2001. Naive CTLs require a single brief period of antigenic stimulation for clonal expansion and differentiation. *Nat. Immunol.* 2: 423–429.
54. Kaech, S. M., and R. Ahmed. 2001. Memory $CD8^+$ T cell differentiation: initial antigen encounter triggers a developmental program in naive cells. *Nat. Immunol.* 2: 415–422.
55. Barouch-Bentov, R., E. E. Lemmens, J. Hu, E. M. Janssen, N. M. Droin, J. Song, S. P. Schoenberger, and A. Altman. 2005. Protein kinase C-θ is an early survival factor required for differentiation of effector $CD8^+$ T cells. *J. Immunol.* 175: 5126–5134.
56. Marsland, B. J., C. Nembrini, N. Schmitz, B. Abel, S. Krautwald, M. F. Bachmann, and M. Kopf. 2005. Innate signals compensate for the absence of PKC-θ during in vivo $CD8^+$ T cell effector and memory responses. *Proc. Natl. Acad. Sci. USA* 102: 14374–14379.
57. Dower, N. A., S. L. Stang, D. A. Bottorff, J. O. Ebinu, P. Dickie, H. L. Ostergaard, and J. C. Stone. 2000. RasGRP is essential for mouse thymocyte differentiation and TCR signaling. *Nat. Immunol.* 1: 317–321.
58. Priatel, J. J., S. J. Teh, N. A. Dower, J. C. Stone, and H. S. Teh. 2002. RasGRP1 transduces low-grade TCR signals which are critical for T cell development, homeostasis, and differentiation. *Immunity* 17: 617–627.
59. Murre, C. 2005. Helix-loop-helix proteins and lymphocyte development. *Nat. Immunol.* 6: 1079–1086.
60. Bain, G., C. B. Cravatt, C. Loomans, J. Alberola-Ila, S. M. Hedrick, and C. Murre. 2001. Regulation of the helix-loop-helix proteins, E2A and Id3, by the Ras-ERK MAPK cascade. *Nat. Immunol.* 2: 165–171.
61. Cannarile, M. A., N. A. Lind, R. Rivera, A. D. Sheridan, K. A. Camfield, B. B. Wu, K. P. Cheung, Z. Ding, and A. W. Goldrath. 2006. Transcriptional regulator Id2 mediates $CD8^+$ T cell immunity. *Nat. Immunol.* 7: 1317–1325.
62. Sabbagh, L., C. C. Srokowski, G. Pulle, L. M. Snell, B. J. Sedgmen, Y. Liu, E. N. Tsitsikov, and T. H. Watts. 2006. A critical role for TNF receptor-associated factor 1 and Bim down-regulation in CD8 memory T cell survival. *Proc. Natl. Acad. Sci. USA* 103: 18703–18708.
63. Dijkers, P. F., R. H. Medema, J. W. Lammers, L. Koenderman, and P. J. Coffer. 2000. Expression of the pro-apoptotic Bcl-2 family member Bim is regulated by the forkhead transcription factor FKHR-L1. *Curr. Biol.* 10: 1201–1204.
64. Asada, S., H. Daitoku, H. Matsuzaki, T. Saito, T. Sudo, H. Mukai, S. Iwashita, K. Kako, T. Kishi, Y. Kasuya, and A. Fukamizu. 2007. Mitogen-activated protein kinases, Erk and p38, phosphorylate and regulate Foxo1. *Cell. Signal.* 19: 519–527.
65. Yang, J. Y., C. S. Zong, W. Xia, H. Yamaguchi, Q. Ding, X. Xie, J. Y. Lang, C. C. Lai, C. J. Chang, W. C. Huang, et al. 2008. ERK promotes tumorigenesis by inhibiting FOXO3a via MDM2-mediated degradation. *Nat. Cell Biol.* 10: 138–148.